Chemical Research in Toxicology

Article

pubs.acs.org/crt

Cross-Linking of Thioredoxin Reductase by the Sulfur Mustard Analogue Mechlorethamine (Methylbis(2-chloroethyl)amine) in Human Lung Epithelial Cells and Rat Lung: Selective Inhibition of Disulfide Reduction but Not Redox Cycling

Yi-Hua Jan,[†] Diane E. Heck,[‡] Rama Malaviya,[§] Robert P. Casillas,[∥] Debra L. Laskin,[§] and Jeffrey D. Laskin*,[†]

[†]Department of Environmental and Occupational Medicine, Rutgers University-Robert Wood Johnson Medical School, Piscataway, New Jersey 08854, United States

[‡]Department of Environmental Health Science, New York Medical College, Valhalla, New York 10595, United States

[§]Department of Pharmacology and Toxicology, Rutgers University, Piscataway, New Jersey 08854, United States

[∥]MRIGlobal, Kansas City, Missouri 64110, United States

Supporting Information

ABSTRACT: Oxidative stress plays a key role in mechlorethamine (methylbis(2-chloroethyl)amine, HN2) toxicity. The thioredoxin system, consisting of thioredoxin reductase (TrxR), thioredoxin, and NADPH, is important in redox regulation and protection against oxidative stress. HN2 contains two electrophilic side chains that can react with nucleophilic sites in proteins, leading to changes in their structure and function. We report that HN2 inhibits the cytosolic (TrxR1) and mitochondrial (TrxR2) forms of TrxR in A549 lung epithelial cells. TrxR exists as homodimers under native conditions; monomers can be detected by denaturing and reducing SDS-PAGE followed by western blotting. HN2 treatment caused marked decreases in TrxR1 and TrxR2 monomers along with increases in dimers and oligomers under reducing conditions, indicating that HN2 cross-links TrxR. Cross-links were also observed in rat lung after HN2 treatment. Using purified TrxR1, NADPH reduced, but not oxidized, enzyme was inhibited and cross-linked by HN2. LC−MS/MS analysis of TrxR1 demonstrated that HN2 adducted cysteine- and selenocysteine-containing redox centers forming monoadducts, intramolecule and intermolecule cross-links, resulting in enzyme inhibition. HN2 cross-links two dimeric subunits through intermolecular binding to cysteine 59 in one subunit of the dimer and selenocysteine 498 in the other subunit, confirming the close proximity of the N- and C-terminal redox centers of adjacent subunits. Despite cross-linking and inhibition of TrxR activity by HN2, TrxR continued to mediate menadione redox cycling and generated reactive oxygen species. These data suggest that disruption of the thioredoxin system contributes to oxidative stress and tissue injury induced by HN2.

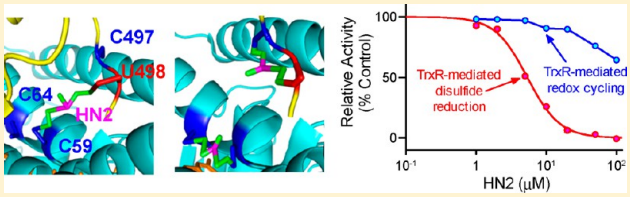

INTRODUCTION

The thioredoxin system, which consists of thioredoxin reductase (TrxR), thioredoxin, and NADPH, plays a crucial role in cellular antioxidant defense.[1] Three isoforms of TrxR have been identified in mammalian cells, including cytosolic (TrxR1) and mitochondrial (TrxR2) forms as well as a testis-specific isoform (TrxR3).[2] All mammalian TrxRs are homodimeric flavoproteins that catalyze the reduction of oxidized thioredoxin as well as other redox-active proteins including glutaredoxin 2 and protein disulfide isomerase, small molecules like 5,5′-dithiobis(2-nitrobenzoic acid) (DTNB), and hydrogen peroxide (H_2O_2).[1,2] Thioredoxin itself functions as a disulfide reductase for a variety of enzymes, many of which are important in the control of DNA synthesis, antioxidant defense, signal transduction, and protein folding.[1] Disruption of the thioredoxin system can suppress these processes, presumably via its requirement for enzymes dependent on thioredoxin including methionine sulfoxide reductases, peroxiredoxins, and ribonucleotide reductases.[1,3,4] TrxRs also mediate chemical redox cycling, a process by which redox active compounds are enzymatically reduced to radical anions.[5−7] Once formed, these free radicals reduce molecular oxygen to form superoxide anion and regenerate the uncharged parent compound. Superoxide anion rapidly dismutates to H_2O_2 and, in the presence of redox active metals, forms highly toxic hydroxyl radicals. Thus, in the presence of redox-active chemicals such as paraquat, various quinones, and nitroaromatic compounds, TrxR can generate reactive oxygen species, contributing to drug-induced oxidative stress and toxicity.[5−9]

A number of electrophilic compounds have been identified as inhibitors of the thioredoxin system. These include alkylating

Received: September 9, 2013
Published: November 26, 2013

   dx.doi.org/10.1021/tx400329a | *Chem. Res. Toxicol.* 2014, 27, 61−75

agents such as nitrosoureas, chlorambucil, melphalan, and cyclophosphamide[10,11] as well dinitrohalobenzenes,[12] quinones,[5] aldehydes such as 4-hydroxynonenal and acrolein,[13,14] metals like arsenic, chromium, mercuric, and organic mercuric compounds,[15−17] and cyclopentenone prostaglandins.[18] Many of these compounds can directly modify either TrxR or thioredoxin; cysteine residues have been identified as critical targets.[12,13,15,17] TrxR is unique in that it is a selenoprotein containing a C-terminus cysteine−selenocysteine redox pair.[19] Selenol has a relatively low pK_a of 5.2, and at physiological pH, selenocysteine is ionized to a highly nucleophilic cysteinyl−selenol.[20,21] Both C-terminal cysteine and selenocysteine adducts have been identified after the reaction of TrxR with electrophiles including 1-chloro-2,4-dinitrobenzene, 4-hydroxynonenal, curcumin, and arsenic trioxide.[12,13,15,22] Although TrxR is a target for nitrosoureas, chlorambucil, melphalan, and mechlorethamine,[10,23] the molecular mechanisms mediating TrxR inhibition have not been elucidated.

Sulfur mustard (2,2′-dichlorodiethyl sulfide) is a potent vesicant that has been used as a chemical-warfare agent. A major target for sulfur mustard is the lung, and most deaths from acute exposure are due to pulmonary damage.[24] Pathological responses in humans include bronchial mucosal injury, inflammation, and fibrosis.[24] In earlier studies, we demonstrated that TrxR is a target for 2-chloroethyl ethyl sulfide (CEES), a monofunctional analogue of sulfur mustard, in lung epithelial cells.[25] Sulfur mustard is a bifunctional alkylating agent with restricted use. In the present studies, we determined if mechlorethamine (methylbis(2-chloroethyl)-amine; HN2), a bifunctional alkylating agent structurally homologous to sulfur mustard and commonly used in cancer chemotherapy,[26] exerts similar cytotoxic effects on TrxR. We found that TrxR was significantly more sensitive to HN2 when compared to CEES; moreover, HN2 alkylated catalytic residues in both the N- and C-terminal redox motif of the enzyme, resulting in enzyme cross-linking. This resulted in inhibition of TrxR-catalyzed disulfide reductase activity but not chemical redox cycling, suggesting that these reactions are mediated by distinct mechanisms. These data demonstrate that TrxR is a target for vesicants and that inhibition of the enzyme in lung cells may be important in oxidative stress and tissue injury.

EXPERIMENTAL PROCEDURES

Chemicals and Enzymes. Purified rat liver TrxR, NADPH, DTNB, menadione, catalase, superoxide dismutase, phosphatase inhibitor (catalog no. P2850, which contains microcystinLR, cantharidin, and (−)-*p*-bromotetramisole) and protease inhibitor cocktail (catalog no. P2714, which contains 4-(2-aminoethyl)-benzenesulfonyl fluoride, E-64, bestatin, leupeptin, aprotinin, and EDTA), and *β*-actin monoclonal antibody were purchased from Sigma (St. Louis, MO). Mechlorethamine hydrochloride was from Aldrich (Milwaukee, WI). Human TrxR mutant (Sec498Cys) was from Ab Frontier (Seoul, Korea). *N*-(Biotinoyl)-*N*′-(iodoacetyl) ethylenediamine (BIAM), Amplex Red reagent, Dulbecco's modified Eagle's medium (DMEM), fetal bovine serum, and penicillin/streptomycin were from Life Technologies (Grand Island, NY). Horseradish peroxidase (HRP)-conjugated streptavidin was from GE Healthcare (Piscataway, NJ). Anti-TrxR1, -TrxR2, and -cytochrome c antibodies were from Santa Cruz (Santa Cruz, CA). Chemiluminescent (ECL) substrate was from Thermo Scientific (Rockford, IL).

Caution: *These chemicals are dangerous.* HN2 is a highly toxic vesicant, and precautions must be taken for its handling, preparation, and animal instillation. Double gloves, safety glasses, masks, and other protective equipment should be used to prevent exposure. Instillations were performed in a designated room under a chemical hood. The HN2 waste was disposed of following Rutgers University Environmental Health and Safety guidelines.

Animal Treatments and Tissue Collection. Male Wistar rats (225−250 g) were purchased from Harlan Laboratories (Indianapolis, IN) and maintained in an AALAC-approved animal care facility. Animals were housed in filter top microisolation cages and provided food and water ad libitum. Animals received humane care in compliance with the guidelines outlined in the Guide for the Care and Use of Laboratory Animals, published by the National Institutes of Health. Rats were treated with PBS (137 mM KCl, 2.7 mM KCl, 10 mM Na_2HPO_4, 2 mM KH_2PO_4, pH 7.4) or HN2 (0.125 mg/kg) by intratracheal instillation as previously described.[27] HN2 was prepared immediately before administration in PBS. All animals appeared clinically normal following instillation with HN2. Animals were euthanized by ip injection of Nembutal (250 mg/kg) 1 d after administration of HN2 or PBS control. Lung lobes were perfused with PBS, removed, and stored at −80 °C.

Cell Culture and Treatments. Human A549 lung cells were obtained from the American Type Culture Collection (Manassas, VA). Cells were grown in DMEM supplemented with 10% fetal bovine serum, 100 units/mL of penicillin, and 100 *μ*g/mL of streptomycin in a humidified atmosphere of 5% CO_2 at 37 °C. Solutions of HN2 were prepared fresh immediately before use in serum-free DMEM.

Cell viability was determined using alamarBlue (BioSource International, Camarillo, CA) as previously described.[25] In brief, A549 cells were seeded into 96-well plates (1.2×10^4 cells/well). After overnight incubation, the cells were rinsed and incubated in serum-free DMEM in the absence or presence of increasing concentrations of HN2 (0.25−500 *μ*M). AlamarBlue (5%) diluted in serum-free DMEM was added to the cultures 24 h later. AlamarBlue reduction was assessed by fluorescence (excitation and emission wavelengths of 555 and 590 nm, respectively) using a SpectraMax M5 spectrofluorometer (Molecular Devices, Sunnyvale, CA) 4 h later. Viability was expressed as the percentage of dye reduction in the presence of HN2 relative to vehicle control. The concentration of HN2 inhibiting cell viability by 50% was 25.3 *μ*M after 24 h treatment.

For preparation of subcellular fractions, A549 cells (5×10^6) were cultured overnight in 15 cm dishes. Cells were rinsed and incubated with increasing concentrations of HN2 (1−50 *μ*M) or vehicle control. Twenty-four hours later, cells were washed twice with ice-cold PBS and removed from the dishes with a cell scraper. After centrifugation (800*g*, 5 min), cell pellets were collected.

Preparation of Cytosol and Mitochondria. Lung and A549 cells were washed with ice-cold 0.9% NaCl and homogenized in Tris buffer (20 mM Tris, 20 mM 3-(*N*-morpholino)propanesulfonic acid, 1 mM EGTA, 100 mM glucose, pH 7.4) containing protease and phosphatase inhibitors using a Teflon homogenizer. The homogenates were centrifuged at 800*g* for 10 min at 4 °C; supernatants were then centrifuged at 9000*g* for 20 min to sediment mitochondria. The resulting supernatants, designated as the S9 fractions, contained cytosolic proteins. Pellets from A549 cells were washed twice with homogenization buffer and then sonicated in homogenization buffer to obtain the mitochondrial fractions. Protein concentrations were determined using a BCA protein assay kit (Thermo Scientific) with bovine serum albumin as a standard.

TrxR Enzyme Assays. TrxR enzyme activity was assayed using DTNB as a substrate according to Holmgren and Bjornstedt[28] with minor modifications. Assay mixtures contained 25 *μ*g of cytosolic fractions or 25−100 nM purified TrxR, 1 mM EDTA, 50 mM KCl, 0.2 mg/mL bovine serum albumin, and 0.25 mM NADPH in a final volume of 100 *μ*L in 50 mM potassium phosphate buffer (pH 7.0). The reaction was initiated by the addition of DTNB (2.5 mM), and increases in absorbance at 412 nm were monitored. Background TrxR-independent reduction of DTNB in cytosolic fractions, determined in the presence of aurothiomalate (0.2 mM), was subtracted from each value. TrxR activity was defined as micromoles of thionitrobenzoic acid formed per minute per milligram of protein using a molar extinction coefficient for thionitrobenzoic acid of 13.6 mM^{-1} min^{-1}.

For studies using purified TrxR enzymes, TrxR was reduced with NADPH (0.25 mM) at room temperature in 50 mM potassium

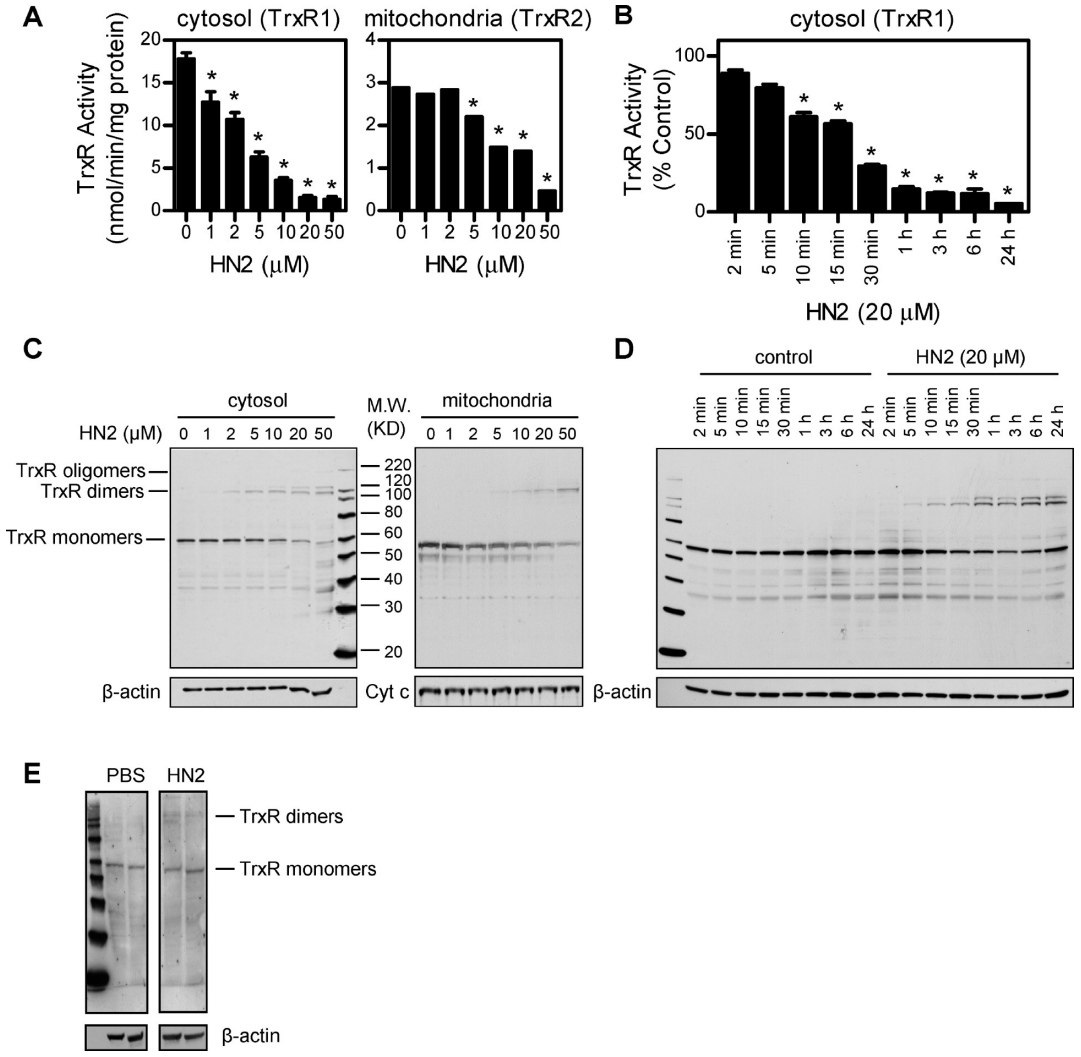

Figure 1. Effects of HN2 on TrxR in A549 cells and rat lungs. Cells were incubated in serum-free medium with increasing concentrations of HN2 or vehicle control. (A–D) After 24 h, subcellular fractions were prepared and analyzed for TrxR1 or TrxR2 enzyme activity using the DTNB assay (A, B) and protein expression by denaturing SDS-PAGE followed by western blotting (C, D). Cytochrome c (Cyt c) and β-actin were used as protein loading controls for mitochondrial and cytosolic fractions, respectively. (A, C) Effects of increasing concentrations of HN2 on TrxR expression and enzyme activity in cytosolic and mitochondrial fractions of A549 cells. (B, D) Time-dependent effects of HN2 on TrxR from cytosolic fractions (TrxR1). Activity is presented as percentage inhibition relative to vehicle-treated controls. Data are expressed as the mean ± SE (n = 3). * indicates significantly different ($p < 0.05$) from vehicle-treated control. (E) Effects of HN2 on TrxR1 cross-linking in rat lungs. Wistar rats were treated with 0.125 mg/kg HN2 or PBS by intratracheal instillation. After 24 h, lungs were collected, cytosolic fractions were prepared, and TrxR1 expression was assayed by western blotting. Each lane represents one lung sample from a single experiment.

phosphate buffer, pH 7.0, 1 mM EDTA, and 50 mM KCl. After 5 min, HN2 (0.1–1000 μM) or control was added, and the reaction mixture incubated for an additional 30 min. The ability of HN2 to inhibit TrxR activity was then determined using the DTNB assay. For studies on the reversibility of TrxR inhibition, reaction mixtures containing HN2-modified TrxR were purified using Chroma Spin TE-10 columns (Clontech, Mountain View, CA) to remove unreacted HN2. Modified TrxR was then analyzed for enzyme activity using the DTNB assay.

BIAM Labeling of TrxR and Western Blotting. HN2-modified TrxR, purified as described above, was incubated in the dark with 50 μM BIAM (dissolved in 50 mM Tris-HCl buffer at pH 6.5 or 8.5) at 37 °C for 30 min. BIAM-labeled protein was denatured in Laemmli sample buffer (Bio-Rad, Hercules, CA) containing 2-mercaptoethanol, analyzed by gel electrophoresis on 10.5–14% polyacrylamide gels (Criterion XT Tris-HCl gels, Bio-Rad), and electroblotted onto nitrocellulose membranes. The extent of BIAM labeling of TrxR was analyzed using HRP-conjugated streptavidin and ECL detection. After BIAM analysis, the blots were stripped, and the membranes reprobed with antibody against TrxR (Santa Cruz) for analysis of total TrxR protein loading. Densitometric analysis of bands on the membranes was performed using a FluorChem Image System (Alpha Innotech, San Leandro, CA).

Analysis of TrxR-HN2 Adducts by LC–MS/MS. NADPH-reduced rat TrxR1 (1 μM) was incubated with or without HN2 (200 μM) at room temperature in a final volume of 100 μL in 50 mM potassium phosphate, pH 7.0, 1 mM EDTA, and 50 mM KCl. After 1 h, the incubation mixture was desalted with Chroma Spin TE-10 columns to remove unreacted HN2. Five microliters of the filtered solution was analyzed for TrxR activity using the DTNB assay. Aliquots of filtered solution (20 μL) were then subjected to SDS-PAGE on 10.5–14% gels. After staining with Coomassie blue, bands containing TrxR were cut from the gels, disulfide bonds were reduced with 20 mM DTT for 1 h at 60 °C, and unmodified thiol/selenol groups were alkylated with 40 mM iodoacetamide for 30 min in the dark at room temperature. TrxR in the gels was then digested with trypsin (Roche, Indianapolis, IN) as previously described.[25] Subsequently, digested peptides were extracted from the gels with 100 μL of formic acid/water/acetonitrile (5:35:60, v/v/v) and dried in a

dx.doi.org/10.1021/tx400329a | Chem. Res. Toxicol. 2014, 27, 61–75

SpeedVac concentrator. Peptides were reconstituted in 0.1% TFA and analyzed by LC−MS/MS on a Dionex U3000 RSLC nano system (Dionex, Sunnyvale, CA) online with a Thermo LTQ Orbitrap Velos mass spectrometer (Thermo Fisher Scientific, San Jose, CA). The peptide mixtures were loaded onto an Acclaim PepMAP 100 nano trap column (5 μm particle, 100 Å pore size, 100 μm × 2 cm, Dionex) and washed for 5 min with solvent A (0.1% formic acid in water) at a flow rate of 10 μL/min. Separation was achieved with an Acclaim PepMAP RSLC nano column (2 μm particle, 100 Å pore size, 75 μm × 15 cm, Dionex) with a 30 min gradient from 2 to 45% of solvent B (0.1% formic acid in acetonitrile) at a flow rate of 300 nL/min. The effluent from the HPLC column was then analyzed by electrospray ionization mass spectrometry. MS spectra were acquired in the Orbitrap with resolution setting at 60 000. MS/MS spectra were acquired in LTQ using a data-dependent acquisition procedure with a cyclic series of a full scan followed by MS/MS scans of the most intense 20 ions with a repeat count of two and the dynamic exclusion duration of 30 s. The MS/MS data were searched via the SEQUEST algorithm against the rat International Protein Index (IPI) database with 10 ppm and 0.8 Da for MS and MS/MS tolerances, respectively. S-Carbamidomethylation at cysteine (+57.021 Da), HN2-induced alkylation at cysteine, lysine, histidine, arginine, and tyrosine (+ 83.073 and +101.084 Da for intrapeptide cross-link and hydroxylated monoadduct, respectively), and oxidation at methionine (+ 15.995 Da) were set as dynamic modifications to identify spectra of adducted peptides. The selection of non-thiol-containing amino acids was based on earlier studies showing that these amino acids were alkylated by HN2 and potential nucleophilic residues for modification by electrophiles.[29,30] Modifications on selenium-containing peptides were searched manually by distinctive isotope patterns and confirmed by the critical b and y ions in the MS/MS. The MS/MS data from ETD fragmentation were also searched against the rat IPI database using the ZCore algorithm, with similar modification settings as the SEQUEST search. The sequence coverage of TrxR tryptic peptides was between 40 and 60% of total TrxR sequence for individual analysis activated by CID or ETD and 72% in combination of both methods.

Assays for NADPH Oxidation and Redox Cycling Activity by TrxR. Oxidation of NADPH in reaction mixes was determined by measuring decreases in absorbance at 340 nm and quantified using an extinction coefficient of 6.2 mM^{-1} cm^{-1}. Reaction mixes consisted of 100 nM TrxR, 0.25 mM NADPH, 1 mM EDTA, 50 mM KCl, and 50 mM potassium phosphate buffer (pH 7.0) in the presence and absence of HN2 (5−200 μM) in a total volume of 100 μL. The same reaction mix without HN2 was used as a control. To analyze the effect of HN2-adducted TrxR on the production of reactive oxygen species, reactions were run in the presence of 100 μM menadione, a quinone known to actively redox cycle with TrxR.[5] Superoxide anion was measured using the superoxide dismutase (SOD)-inhibitable acetylated cytochrome c reduction assay.[31] Reactions were run in a total volume of 100 μL and contained 250 nM TrxR, 300 mM potassium phosphate buffer, pH 7.8, 0.1 mM EDTA, 0.25 mM NADPH, HN2 (5−200 μM) or control, and 100 μM acetylated cytochrome c. Cytochrome c reduction was monitored at room temperature by increases in absorption at 550 nm and quantified using an extinction coefficient of 21.1 mM^{-1} cm^{-1}. Reaction mixtures containing 2000 units/mL of SOD were used as controls.

H_2O_2 was measured using either the Amplex Red assay[7] or by its conversion to hydroxyl radicals in the presence of ferrous ion using the terephthalate assay.[32] For Amplex Red assays, reactions were run in a total volume of 100 μL in 50 mM potassium phosphate buffer, pH 7.8, 0.25 mM NADPH, 1 unit/mL HRP, HN2 (5−200 μM) or control, and 50 μM Amplex Red reagent. Product formation was assessed fluorometrically using excitation and emission wavelengths of 530 and 587 nm, respectively. To measure hydroxyl radicals, the reaction was supplemented with 1 mM terephthalate and Fe^{2+} (100 μM)/EDTA (110 μM) complex in place of Amplex Red and HRP. After 30 min incubation at 37 °C, the reaction was terminated by the addition of an equal volume of ice-cold methanol. After centrifugation at 20 000 g for 10 min, the supernatant was analyzed for 2-hydroxyterephthalate by reverse-phase HPLC as previously described.[32]

Molecular Modeling and Data Analysis. The 3D model of the rat TrxR/HN2 was generated using PyMOL software.[33] The crystal structure of rat TrxR1 with a reduced C-terminal tail was obtained from the Protein Data Bank (PDI ID: 3EAN).[34] TrxR activity, NADPH oxidation, and H_2O_2 formation were monitored over 30 min, and the initial velocities were analyzed using SoftMax Pro software (Molecular Devices, Sunnyvale, CA). IC_{50} values were determined by the nonlinear regression method of curve fitting using Prism 5 software (GraphPad Inc., San Diego, CA). Data were analyzed using the Student's t test. A value of $p < 0.05$ was considered significant.

RESULTS

Effects of HN2 on Thioredoxin Reductase in Lung Epithelial Cells and Rat Lung. In initial experiments, we examined the effects of HN2 on TrxR in A549 lung epithelial cells. HN2 caused a concentration- and time-dependent inhibition of enzyme activity (Figure 1A,B). Cytosolic thioredoxin reductase (TrxR1) was more sensitive to HN2 than the mitochondrial enzyme (TrxR2). Maximal inhibition was observed after 24 h; at this time, the IC_{50} for inhibition was 2.7 μM for cytosolic TrxR1 and 14.3 μM for mitochondrial TrxR2. Immunoblot analysis of subcellular fractions of control cells on denaturing SDS polyacrylamide gels showed TrxR monomers ($M_w \approx 57$ kDa); both TrxR1 and TrxR2 had similar mobilities on the gels (Figure 1C). Following HN2 treatment, cross-linked TrxR dimers ($M_w = 114$ kDa) and oligomers ($M_w \geq 130$ kDa) appeared, with a corresponding decrease in TrxR monomers. In addition, doublet TrxR dimers were evidenced at higher HN2 concentrations (HN2 ≥ 20 μM), suggesting that HN2 also cross-linked TrxR and other protiens. Consistent with inhibition of enzyme activity, HN2 was less efficient at cross-linking TrxR2 when compared to TrxR1. Cross-linking of TrxR was concentration- and time-dependent for both the cytosolic and mitochondrial forms of the enzyme (Figure 1C,D and data not shown). TrxR cross-linking was observed within 5 min and persisted for at least 24 h. The effects of HN2 on TrxR1 was further assessed in rat lungs following intratracheal instillation of HN2 (0.125 mg/kg, 24 h) or PBS control. Using cytosolic fractions from the tissue, TrxR1 monomers were detected in both HN2-treated and control animals. TrxR1 dimers were only detected in lungs from HN2-treated rats (Figure 1E). These data indicate that HN2 cross-linked TrxR1 in vivo.

Effects of HN2 on Purified TrxR1. Mechanisms mediating inhibition of TrxR by HN2 were examined next using purified rat liver TrxR1. Several inhibitors of TrxR have been shown to be dependent on the redox status of the enzyme.[22,35] The effects of TrxR redox status on enzyme inhibition by HN2 was investigated by preincubating the enzyme with NADPH. As shown in Figure 2A, HN2 had no significant effect on TrxR activity in the absence of NADPH pretreatment. In contrast, a marked inhibition of enzyme activity was observed when TrxR was reduced by NADPH (50 and 250 μM). Reduced TrxR was required at all concentrations of HN2 tested (5−50 μM). These data indicate that inhibition of TrxR by HN2 is dependent on the redox status of TrxR and that reduction of TrxR is required for HN2-induced inactivation. The IC_{50} value for inhibition of purified TrxR by HN2 was 5.4 ± 0.22 μM (mean ± SE, $n = 3$). Inhibition of TrxR by HN2 was found to be irreversible. Thus, TrxR activity could not be recovered even after separating free HN2 in reaction mixtures using Chroma Spin TE-10 columns (Figure 2C). The effects of HN2 on human TrxR1 and on a recombinant mutant form of human TrxR1 were also analyzed. Using cytosolic fractions of A549

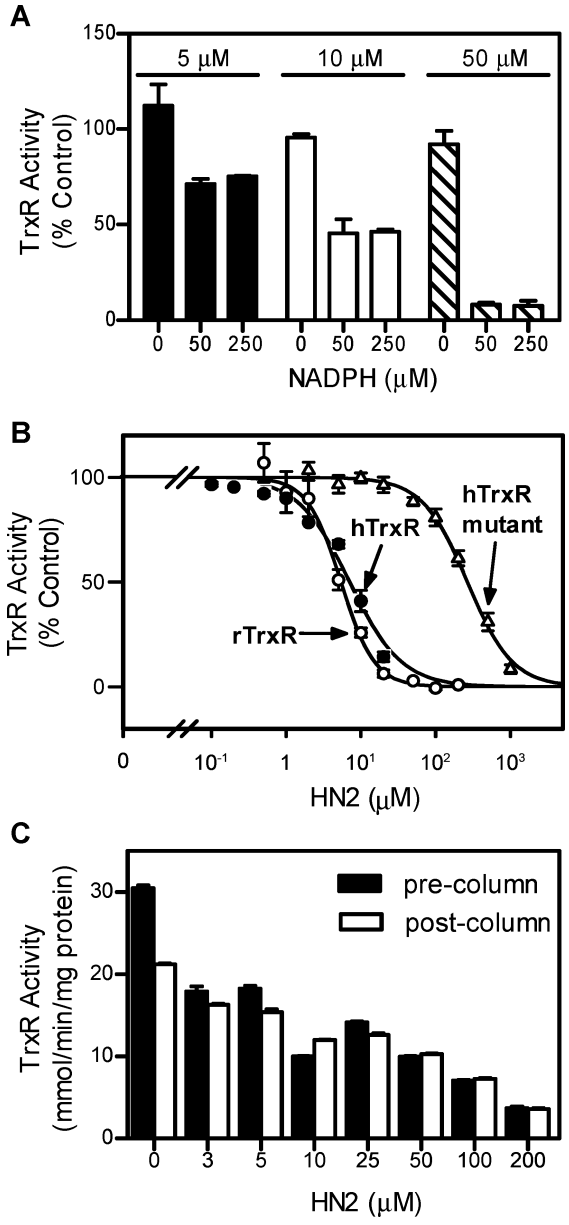

Figure 2. Inhibition of purified TrxR1 by HN2. (A) Effects of TrxR redox state on enzyme inhibition by HN2. Purified rat liver TrxR1 (100 nM) was preincubated without and with increasing concentrations of NADPH at room temperature. After 5 min, HN2 (5, 10, 50 μM) was added to the enzyme reaction mixture. After an additional 30 min, NADPH was added to a final concentration of 250 μM, and TrxR activity was determined by the DTNB assay. Data are expressed as the mean ± SE (n = 3). (B) Effects of increasing concentrations of HN2 on TrxR activity. Rat liver TrxR1 (rTrxR, white circles), human TrxR1 from A549 cells (hTrxR, black circles), or hTrxR1 Sec498Cys mutant enzyme (white triangles) was treated with 250 μM NADPH for 5 min followed by HN2. After 30 min, enzyme activity was assessed. (C) Irreversible inhibition of TrxR1 by HN2. Reduced rat TrxR1 was incubated at room temperature with increasing concentrations of HN2 in the presence of NADPH. After 30 min, TrxR in the reaction mixture was purified using Chroma Spin TE-10 columns to remove unreacted HN2. The remaining TrxR activity was then assessed.

cells, which contain wild-type human TrxR1, HN2 was found to inhibit enzyme activity (IC_{50} = 7.1 ± 0.61 μM); inhibition was similar to the rat enzyme. A human mutant enzyme in which selenocysteine (Sec498) was replaced with cysteine was markedly less sensitive to HN2 (IC_{50} = 270 ± 59 μM), suggesting that the selenocysteine-containing C-terminal is key for enzyme inhibition and that it is a potential target for HN2 alkylation.

Alkylation of the Dithiol and Selenol/Thiol Redox Motifs in TrxR by HN2. Our findings that a mutant TrxR without selenocysteine was less sensitive to HN2 and that HN2 inactivated reduced, but not oxidized, TrxR suggested that HN2 acts by modifying selenocysteine and/or cysteine residues in the enzyme. To investigate this, we used a BIAM labeling technique in which the label selectively reacts with cysteine ($pK_a \approx 8.5$) and/or selenocysteine ($pK_a \approx 5.2$) in TrxR in a pH-dependent manner.[13,21] Whereas at pH 6.5 only −SeH is alkylated by BIAM because of the low pKa (5.2) of selenol on selenocysteine, at pH 8.5, both -SH and -SeH are labeled by BIAM.[13] The labeling efficiency of TrxR by BIAM at pH 6.5 and 8.5 is shown in Figure 3. At pH 6.5, reduction of TrxR by NADPH caused a significant increase in BIAM labeling without HN2 treatment. With oxidized TrxR (not pretreated with NADPH), HN2 had no effect on BIAM labeling. However, with reduced TrxR (pretreated with NADPH), HN2 readily decreased BIAM labeling. Under these conditions, HN2 induced cross-linking, generating both TrxR dimers and oligomers that labeled only weakly with BIAM. These data indicate that selenocysteine is a target for modification by HN2.

At pH 8.5, HN2 caused a small concentration-dependent decrease in BIAM labeling in oxidized TrxR; this occurred without cross-linking and without a loss in enzyme activity, suggesting that HN2 also binds to a cysteine residue that is not critical for TrxR activity. As shown, HN2 caused a marked increase in the formation of TrxR dimers and oligomers, demonstrating cross-linking of reduced TrxR. This was associated with a decrease in BIAM labeling in TrxR monomers, which was due to a decrease in TrxR monomers. However, total BIAM labeling in monomers, dimers, and oligomers decreased following NADPH reduction of the enzyme. These data provide further support for the idea that HN2 reacts with selenocysteine as well as cysteine residues in the enzyme.

Identification of HN2-Alkylated Residues on TrxR. HN2-alkylation sites on TrxR were investigated by ESI LC−MS/MS analysis of tryptic peptides prepared from the modified enzyme. HN2 contains two chloroethyl groups, each of which can react with nucleophilic sites on proteins. Initial alkylation of TrxR by one HN2 chloroethyl group leads to TrxR-HN2 monoadduct(s), which retain an unreacted chloroethyl group. These monoadducts can then react with nucleophilic sites on the same peptide or on a neighboring peptide, leading to the formation of intrapeptide or interpeptide cross-links, respectively (with a mass increase of 83.07 Da). Monoadducts can also react with a water molecule, leading to the formation of hydroxylated HN2 monoadducts (with a mass increase of 101.08 Da). Additionally, unmodified cysteine or selenocysteine residues on protein will be alkylated by iodoacetamide (addition of carbamidomethyl groups; mass increase of 57.02 Da) that is introduced during the in-gel digestion process to protect free thiol/selenol groups on the protein. Table 1 summarizes the observed modified peptides and their assignments from a database search (selective ion chromatograms [SICs], isotopic spectra, and tandem mass spectra of adducted peptides are shown in Figure 4 and in Supporting Information Figures S1−S3). Both monoalkylated adducts and intramolecule cross-links were detected in TrxR, predominantly

dx.doi.org/10.1021/tx400329a | Chem. Res. Toxicol. 2014, 27, 61−75

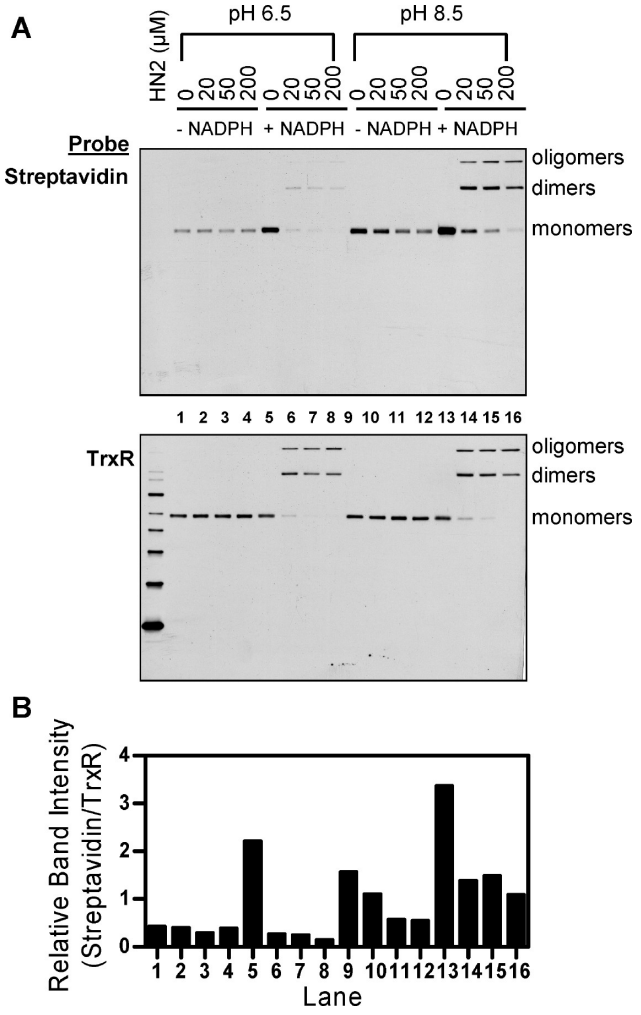

Figure 3. Effects of HN2 on labeling of TrxR by BIAM. Reduced and nonreduced rat TrxR1 was treated with HN2 or vehicle control. After 30 min, HN2-alkylated TrxR1 was purified using Chroma Spin TE-10 columns to remove unbound vesicant and then labeled with BIAM at pH 6.5 or 8.5. Samples were analyzed by western blotting 30 min after labeling. The extent of BIAM labeling on TrxR was evaluated by the specific binding of streptavidin-HRP followed by ECL detection. (A) Western blots showing TrxR probed with streptavidin-conjugated HRP or antibody to TrxR. (B) Densitometric analysis of the labeling efficiency of TrxR by BIAM. The extent of BIAM labeling of TrxR was determined by the relative intensities of the total streptavidin bands to the total TrxR bands.

linked to cysteine residues. Figure 4 shows an example of an HN2-modified peptide from a database search and the sequence assignment of this peptide. This adducted peptide was detected in gel bands representing TrxR monomers, dimers, and oligomers but not in the TrxR control (Figure 4A). The isotopic spectrum revealed that it is a triply charged ion, indicated by the mass difference of 0.33 Da between neighboring peaks, at m/z 529.61 ($[M + H]^+$ 1586.83 Da). The mass of the parent ion is in agreement with the protonated WGLGGTCVNVGCIPK peptide (peptide 53−67; $[M + H]^+$ 1503.74 Da) plus 83.09 Da, corresponding to the WGLGG-TCVNVGCIPK peptide modified by one HN2. The MS/MS spectrum confirmed that one HN2 is covalently bound to cysteine 59 and another to cysteine 64, showing normal y_2^+ and y_3^+ ions and modified b_{12}^{2+}, b_{13}^{2+}, y_{12}^{2+}, y_{13}^{2+}, and y_{14}^{2+} ions with mass increases of 42 Da.

Because standard MS database search engines including SEQUEST and ZCore do not support the observed mass of selenocysteine-containing peptides or two-peptide cross-links, we performed a manual search for these peptides on the basis of the distinct isotope patterns and expected masses of the parent ions with all possible combinations of adducted residues (cysteine, selenocysteine, and lysine). The adducted peptides were further confirmed by critical fragment ions appearing after MS/MS. One selenocysteine-containing intrapeptide and two interpeptide cross-links were identified (Table 2). A doubly charged ion at m/z 614.24 ($[M + H]^+$ 1227.48 Da) was found to agree with the protonated SGGDILQSGCUG peptide ($[M + H]^+$ 1143.44 Da) modified with one HN2 molecule. This adducted peptide was detected in HN2-treated samples including protein bands from gel electrophoresis (monomers, dimers, and oligomers) as well as solution digestion but not in TrxR control samples (Figure 5). The tandem mass spectrum of this ion exhibited a series of normal b ions (b_3^+−b_9^+) and a series of modified y ions (y_3^+−y_9^+) with masses that were 84.04 Da higher than those of the corresponding y ions compared to unmodified SGGDILQSGCUG peptide. These results indicate that HN2 adducted in the last three amino acids in the C-terminus (cysteine 497, selenocysteine 498, and glycine 499), suggesting that HN2 was alkylated to cysteine 497 and selenocysteine 498 in TrxR (Figure 5). In addition, two different charged ions at m/z 712.07 (4+) and 949.09 (3+) were observed that corresponded to the same $[M + H]^+$ value of 2845.27 Da. These data are consistent with the masses of SGGDILQSGCUG peptide (peptide 488−499; $[M + H]^+$ 1143.44 Da) and WGLGGTCVNVGCIPK peptide (peptide 53−67; $[M + H]^+$ 1503.74 Da) with the addition of one HN2 and two carbamidomethyl groups. They were identified in TrxR dimer and oligomer protein bands but not in TrxR monomers or untreated TrxR. Figure 6 shows one of the extracted ion chromatograms at m/z 712.07 and its tandem mass spectrum. Of the fragment ions, $y'_5{}^+$ and $y'_6{}^+$ were observed with masses 57 Da higher than those of the corresponding y′ ions from unmodified WGLGGTCVNVGCIPK peptide, suggesting that there is a carbamidomethylated cysteine at position 64. Thus, HN2 is modifying cysteine 59 on the N-terminal redox center-containing peptide. Fragment ion $y'_2{}^+$ was also consistent with the normal y′ ion from WGLGGTCVNVGCIPK peptide. Furthermore, b_4^+, b_5^+, and b_6^+ ions were consistent with the normal b ions from SGGDILQSGCUG peptide, suggesting that HN2 is modifying one of the last seven residues in the C-terminal of TrxR. Although no direct evidence showing the exact HN2 binding site on the SGGDILQSGCUG peptide was detected, on the basis of its relative reactivity, it is likely that HN2 reacts with selenocysteine 498 on this peptide. These data suggest that HN2 cross-links cysteine 59 in one subunit of TrxR (residues S_{488}GGDILQSGCUG_{499}) and selenocysteine 498 in the other subunit of the enzyme (residues W_{53}GLGGTCVNVGCIPK_{67}), leading to dimer formation. These results confirm that HN2 directly targets redox centers in TrxR.

Effects of HN2 on Chemical Redox Cycling by TrxR. In addition to reducing thioredoxin, TrxR mediates chemical redox cycling in an NADPH-dependent reaction that generates superoxide anion.[36] Superoxide anion rapidly dismutates into H_2O_2 and, in the presence of redox active metals, forms highly toxic hydroxyl radicals. We next determined if HN2 altered the ability of TrxR to mediate redox cycling. In these experiments, we used menadione (2-methyl-1,4-napthoquinone) as the

dx.doi.org/10.1021/tx400329a | Chem. Res. Toxicol. 2014, 27, 61−75

Table 1. HN2-Modified TrxR Peptides Detected by LC−ESI-MS/MS in the Tryptic Digest using a Database Search

peptide sequence	m/z	charge	t_R (min)	$[M + H]^+$	modification[a,b]	activation[c]	protein species[d]
WGLGGTC$_{59}$VNVGC$_{64}$IPK	529.61	3	28.88	1586.83	C$_{59}$−C$_{64}$ HN2 cross-link	CID	monomer
						ETD	dimer
							oligomer
WGLGGTC$_{59}$VNVGC$_{64}$IPK	554.63	3	29.12	1661.86	C$_{59}$ hydroxylated HN2	CID	monomer
					C$_{64}$ carbamidomethylation	ETD	dimer
							oligomer
WGLGGTC$_{59}$VNVGC$_{64}$IPK	554.63	3	29.12	1661.86	C$_{59}$ carbamidomethylation	CID	monomer
					C$_{64}$ hydroxylated HN2	ETD	dimer
							oligomer
YLGIPGDKEYC$_{177}$ISSDDLFSLPYC$_{189}$PGK	741.60	4	35.91	2963.40	C$_{177}$−C$_{189}$ HN2 cross-link	ETD	dimer
							oligomer
C$_{365}$DYDNVPTTVFTPLEYGC$_{382}$C$_{383}$GLSEEK	975.10	3	32.92	2923.29	C$_{365}$ carbamidomethylation	CID	solution
					C$_{382}$−C$_{383}$ HN2 cross-link	ETD	digestion
C$_{365}$DYDNVPTTVFTPLEYGC$_{382}$C$_{383}$GLSEEK	975.10	3	32.92	2923.29	C$_{365}$−C$_{382}$ HN2 cross-link	CID	solution
					C$_{383}$ carbamidomethylation	ETD	digestion
C$_{365}$DYDNVPTTVFTPLEYGC$_{382}$C$_{383}$GLSEEK	975.10	3	32.92	2923.29	C$_{365}$−C$_{383}$ HN2 cross-link	CID	solution
					C$_{382}$ carbamidomethylation	ETD	digestion

[a]On the basis of the MS/MS results. [b]S-Carbamidomethylation on cysteine results from the process of in-gel digestion using iodoacetamide to protect unreacted thiol groups. [c]Fragmentation methods: CID, collision-induced dissociation; ETD, electron transfer dissociation. [d]Adducts were detected in monomers, dimers, and/or oligomers from the protein bands isolated from the SDS-PAGE or solution digestion of reduced TrxR/HN2.

redox cycling chemical. Menadione, but not HN2, was found to readily redox cycle with TrxR and to generate superoxide anion, H_2O_2, and hydroxyl radicals (Figure 7A−C). Accumulation of superoxide anion was inhibited by superoxide dismutase but not catalase, whereas accumulation of H_2O_2 was inhibited by catalase (Figure 7A,B). Hydroxyl radical production was inhibited by catalase and DMSO, a hydroxyl radical trap (Figure 7C and data not shown). Consistent with the requirement for NADPH in the redox cycling reaction,[36] we found an increase in NADPH utilization in enzyme assays (Figure 7D).

The mechanisms of TrxR-mediated menadione redox cycling were further characterized using TrxR prealkylated with increasing concentrations of HN2. Using rat purified enzyme and under conditions where HN2 caused a marked inhibition of TrxR activity, menadione continued to redox cycle with TrxR, although at reduced rates at higher concentrations (HN2 $\geq$ 50 μM) (Figure 7E). For example, at 20 μM concentrations, HN2 inhibited disulfide reduction by >90%, whereas menadione redox cycling, as measured by H_2O_2 formation in Amplex Red assays, was inhibited by approximately 10% (Figures 2B vs 7E). Human TrxR1 Sec498Cys mutant, which is less active in disulfide reduction and less sensitive to HN2 when compared to rat TrxR1 (Figure 2B), also actively mediated menadione redox cycling, generating reactive oxygen species including H_2O_2 and hydroxyl radicals (Figure 7E and data not shown). This suggests that selenocysteine in the C-terminal redox center of TrxR is not required for menadione redox cycling. HN2 prealkylation of human enzyme displayed only minimal effects on menadione redox cycling, similar to those observed in the rat enzyme (Figure 7E). These data indicate that disulfide reduction and quinone redox cycling by TrxR occur by distinct mechanisms.

DISCUSSION

Bifunctional alkylating agents such as HN2 have the capacity to cross-link cellular macromolecules via a sequence that includes aziridinium formation followed by nucleophilic attack (Figure 8A, mechanism of protein cross-linking).[26] The present studies demonstrate that both TrxR1 and TrxR2 are targets for HN2-forming monoadducts as well as intra- and intermolecular cross-links. This results in irreversible inhibition of TrxR disulfide reductase activity in both human type II lung epithelial cells and highly purified enzyme preparations from rat liver. Intermolecular HN2 adducts can result in the formation of cross-linked TrxR dimers and oligomers by bridging proximal nucleophilic sites on two or multiple subunits or neighboring proteins. LC−MS/MS analysis and pH-dependent iodoacetamide-labeling experiments showed that TrxR inhibition by HN2 involves covalent modification of catalytic residues, both cysteine and selenocysteine, within the N- and C-terminal redox centers of the enzyme. These modifications interfere with the formation of critical dithiol intermediates in the TrxR/thioredoxin reaction, leading to enzyme inactivation. Previously, we demonstrated that TrxR is a target for CEES, a monofunctional sulfur mustard vesicant.[25] HN2 was found to exhibit significantly greater TrxR inhibitory activity when compared to CEES in intact cells (IC_{50} = 2.7 μM vs 1.5 mM). This was correlated with an inhibitory effect on cell viability after vesicant treatment (IC_{50} = 25.3 μM and 6 mM for HN2 and CEES, respectively). By contrast, in vitro studies using purified rat TrxR1 showed that HN2 and CEES inhibited TrxR with similar potency (IC_{50} = 5.4 and 4.6 μM for HN2 and CEES, respectively).[25] The differential effects on TrxR inhibition between cell culture and purified enzyme suggest that other factors, including bioavailability of the vesicants, may play a role in mediating changes in cell viability and inhibition of purified TrxR. These data indicate that TrxR mediates, at least in part, the actions of HN2. This could be due to increased oxidative stress following HN2 treatment; alternatively, TrxR1 reduction may lead to suppressed DNA synthesis and repair. TrxRs are key enzymes in thiol redox control, a process regulating many cellular functions including resistance to oxidative stress, ribonucleotide reduction, and transcription factor modulation.[1,2] Our findings that HN2 targets these enzymes may be an important mechanism of HN2-induced oxidative stress and tissue injury.

dx.doi.org/10.1021/tx400329a | Chem. Res. Toxicol. 2014, 27, 61−75

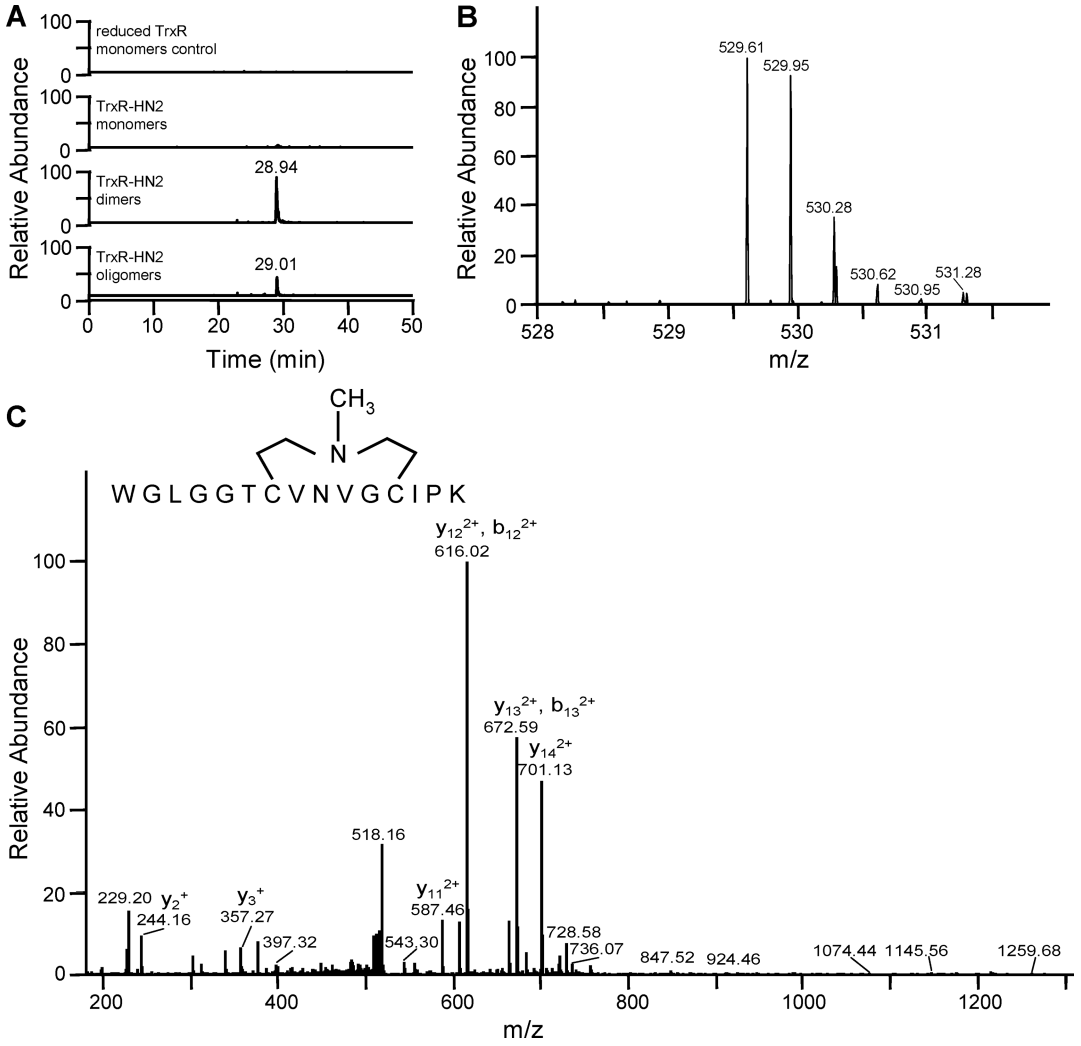

Figure 4. LC−MS/MS analysis of HN2-adducted TrxR tryptic peptide at m/z 529.61. Reduced-rat TrxR1 (1 μM) was incubated with or without HN2 (200 μM) at room temperature. After 1 h, the reaction mixture was desalted, and the HN2-modified protein was further purified by SDS-PAGE. The purified protein was reduced with DDT, reacted with iodoacetamide, and digested with trypsin in the gel. The resulting peptides were analyzed using LC−MS/MS. (A) Extracted ion chromatograph showing the specific peak detected in HN2-treated samples but not in control samples. A small but consistent band detected in monomers resulted from much less protein in the monomers, compared to dimers and oligomers, after HN2 cross-linking. The protein content is about 20% in monomers when compared to dimers and oligomers, as detected by gel staining with Coomassie blue. (B) Isotopic spectrum of triply charged ion at m/z 529.61. (C) MS/MS spectrum of CID product ions from the HN2-modified tryptic ion at m/z 529.61, z = 3. The peptide sequence was determined to be WGLGGTCVNVGCIPK (residues 53−67 in TrxR) with one intramolecular HN2 cross-link on cysteine 59 and cysteine 64. Matched b and y fragments are marked. Inset shows the sequence assignment of this triply charged ion.

Table 2. HN2-Modified Selenocysteine-Containing Peptides Detected by LC−ESI-MS/MS in the Tryptic Digest

peptide sequence	m/z	charge	t_R (min)	$[M + H]^+$	modification[a,b]	activation[c]	protein species[d]
SGGDILQSGC$_{497}$U$_{498}$G	614.24	2	21.43	1227.48	C$_{497}$−U$_{498}$ HN2 cross-link	CID	monomer
						ETD	dimer
							oligomer
							solution digestion
WGLGGTC$_{59}$VNVGC$_{64}$IPK	712.07	4	31.03	2845.27	C$_{59}$−U$_{498'}$ HN2 cross-link	CID	dimer
SGGDILQSGC$_{497}$U$_{498}$G					C$_{64}$ carbamidomethylation	ETD	oligomer
					C$_{497'}$ carbamidomethylation		solution digestion
WGLGGTC$_{59}$VNVGC$_{64}$IPK	949.09	3	31.03	2845.27	C$_{59}$−U$_{498'}$ HN2 cross-link	CID	dimer
SGGDILQSGC$_{497}$U$_{498}$G					C$_{64}$ carbamidomethylation	ETD	oligomer
					C$_{497'}$ carbamidomethylation		solution digestion

[a]On the basis of the MS/MS results. [b]S-Carbamidomethylation on cysteine results from the process of in-gel digestion using iodoacetamide to protect unreacted thiol groups. [c]Fragmentation methods: CID, collision-induced dissociation; ETD, electron transfer dissociation. [d]Adducts were detected in monomers, dimers, and/or oligomers from the protein bands isolated from the SDS-PAGE or solution digestion of reduced TrxR/HN2.

dx.doi.org/10.1021/tx400329a | Chem. Res. Toxicol. 2014, 27, 61−75

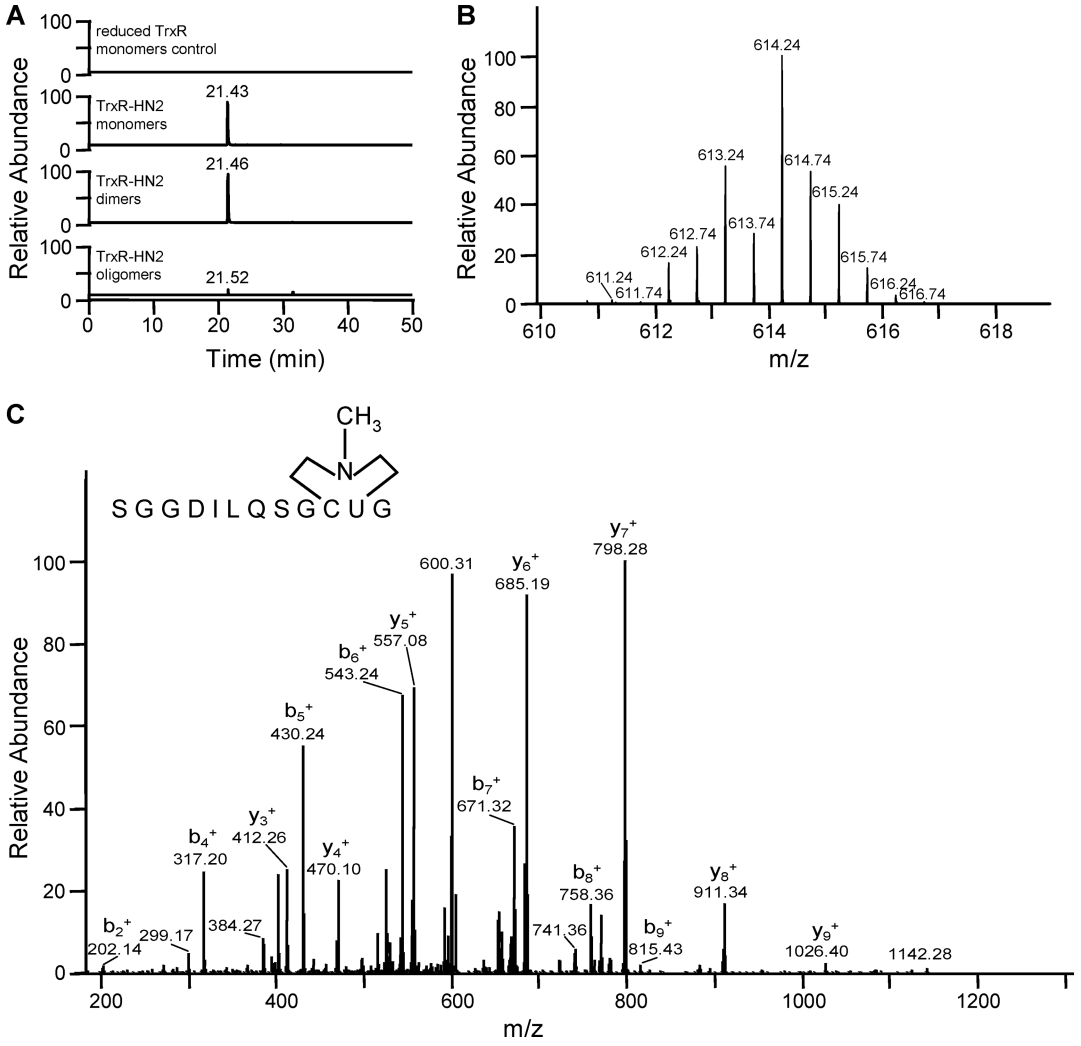

Figure 5. LC–MS/MS analysis of HN2-adducted TrxR tryptic peptide at m/z 614.24. (A) Extracted ion chromatograph showing the specific peak detected in HN2-treated samples but not in control samples. (B) Isotopic spectrum of doubly charged ion at m/z 614.24. (C) MS/MS spectrum of CID product ions from the HN2-modified tryptic ion at m/z 614.24, z = 2. The peptide sequence was determined to be SGGDILQSGCUG (residues 488–499 in TrxR) with one intramolecular HN2 cross-link between cysteine 497 and selenocysteine 498. Matched b and y fragments are marked. Inset shows the sequence assignment of this doubly charged ion.

Human cytosolic TrxR1 and mitochondrial TrxR2 are structural homologous selenoproteins with similar catalytic mechanisms.[2] We found that both TrxR1 and TrxR2 are molecular targets for HN2, although they displayed differential sensitivities. Thus, TrxR2 was less sensitive to HN2 than TrxR1 with respect to inhibition of enzyme activity. This is likely due to reduced formation of HN2 adducts, as indicated by reduced formation of dimers/oligomers when compared to TrxR1. These data are consistent with previous studies showing that TrxR1 and TrxR2 display different substrate and inhibitor specificities[37,38] and suggest that TrxR1 and TrxR2 may have some distinct biochemical features contributing to these differences. This is supported by analysis of TrxR crystal structures, which showed that the positioning of key residues around the redox centers of TrxR2 is different from TrxR1.[39] Moreover, because of the different cellular localization of these isozymes, it is likely that HN2 concentrations are different in cytosolic and mitochondrial compartments, leading to divergent sensitivities.

Using highly purified rat TrxR, we found that HN2 is only effective when the enzyme is reduced by NADPH. This is consistent with other alkylating and nonalkylating TrxR inhibitors including curcumin, quinols, and CEES.[5,22,25,35] Earlier work suggested that NADPH acts by reducing disulfide and selenenylsulfide in TrxR to highly reactive dithiols and selenolthiol in the N- and C-terminal redox centers of the enzyme. This also triggers conformational changes in the redox centers of the enzyme.[19] This is supported by studies on the crystal structures of selenocysteine-containing rat TrxR1 showing that the oxidized enzyme contains a C-terminal selenenylsulfide motif at a site distant from the N-terminal disulfide motif, which is not optimal for substrate binding, and/or the formation of an electron-transfer complex required for enzyme activity.[34] In the reduced enzyme, the selenocysteine residue turns outward, which is more solvent accessible than the selenenylsulfide redox center in the oxidized enzyme. By triggering conformational changes in the catalytic center of the enzyme, substrate binding and electron transfer during catalysis may be facilitated. Our results indicate that reduced domains in TrxR promote alkylation by HN2 and that cysteine and selenocysteine residues in TrxR are critical for covalent modification by HN2.

dx.doi.org/10.1021/tx400329a | Chem. Res. Toxicol. 2014, 27, 61–75

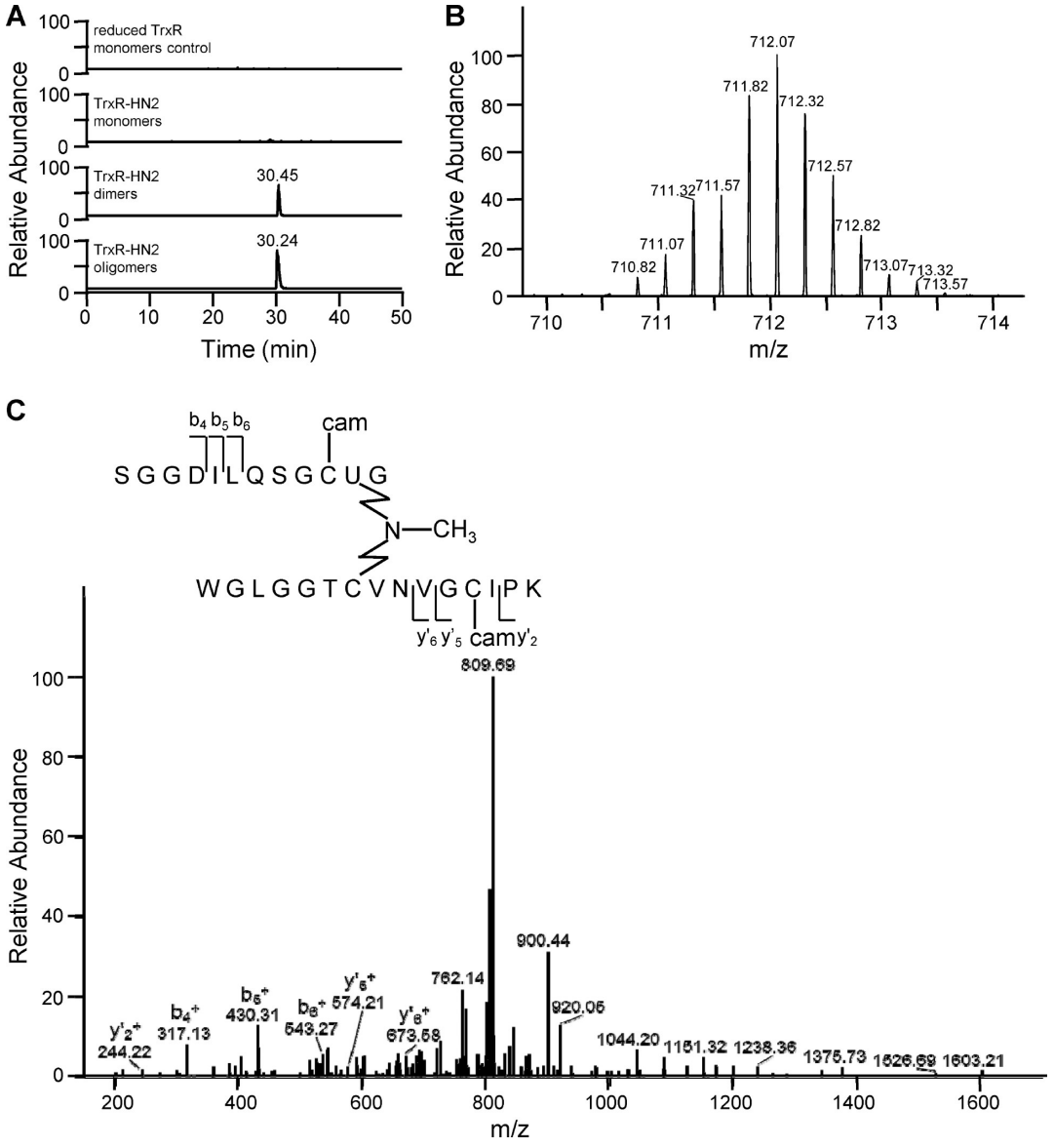

Figure 6. LC–MS/MS analysis of HN2-adducted TrxR tryptic peptide at *m/z* 712.07. (A) Extracted ion chromatograph showing the specific peak detected in HN2-treated samples but not in control samples. (B) Isotopic spectrum of quadruply charged ion at *m/z* 712.07. (C) MS/MS spectrum of CID product ions from the HN2-modified tryptic ion at *m/z* 712.07. It was identified as a quadruply charged ion with one HN2 cross-link and two carbamidomethylated cysteines linking a peptide in one subunit of TrxR (residues S_{488}GGDILQSGCUG$_{499}$) with a peptide in the other subunit of the enzyme (residues W_{53}GLGGTCVNVGCIPK$_{67}$). Matched b and y fragments are marked. Inset shows the sequence assignment of this quadruply charged ion.

Mammalian TrxR is a homodimeric flavoprotein with a head-to-tail arrangement of its two subunits. Each subunit contains an N-terminal redox-active disulfide and a C-terminal redox-active selenenylsulfide in their redox domains. In its active dimeric conformation, the N-terminal redox domain of one subunit is situated in proximity to the C-terminal redox domain of the other subunit. Many TrxR inhibitors have been shown to selectively react with catalytic residues within redox centers of TrxR, resulting in enzyme inhibition.[40] As indicated above, preferential alkylation of TrxR on selenocysteine has been established for several inhibitors, including 4-hydroxynonenal, curcumin, arsenic trioxide, and CEES, presumably because of the low pK_a of selenol and its location in the solvent accessible C-terminal region of the enzyme.[13,15,22,25,35] Our findings that HN2 is an efficient inhibitor of wild-type human and purified rat TrxR, which contain selenocysteine, but not human mutant enzyme (Sec498Cys) lacking selenocysteine, is in accord with the idea that selenocysteine is a dominant target for HN2 modification. This is supported by our iodoacetamide binding experiments showing that HN2 is more effective in blocking BIAM binding at pH 6.5 when compared to pH 8.5. We speculate that by modifying the TrxR catalytic sites, HN2 interferes with the transfer of reducing equivalents to TrxR substrates and/or substrate binding to the enzyme and that this leads to enzyme inhibition. Our LC–MS/MS analysis demonstrates that HN2 covalently modifies catalytic centers by (1) forming monoadducts on cysteine 59 and cysteine 64 in the N-terminal redox center, (2) bridging catalytic residues cysteine 59/cysteine 64 and cysteine 497/selenocysteine 498 in the N- and C-terminal redox centers, respectively, and (3) linking two dimeric subunits through intermolecular binding to cysteine 59 in one subunit of the dimer and selenocysteine 498

dx.doi.org/10.1021/tx400329a | *Chem. Res. Toxicol.* 2014, 27, 61–75

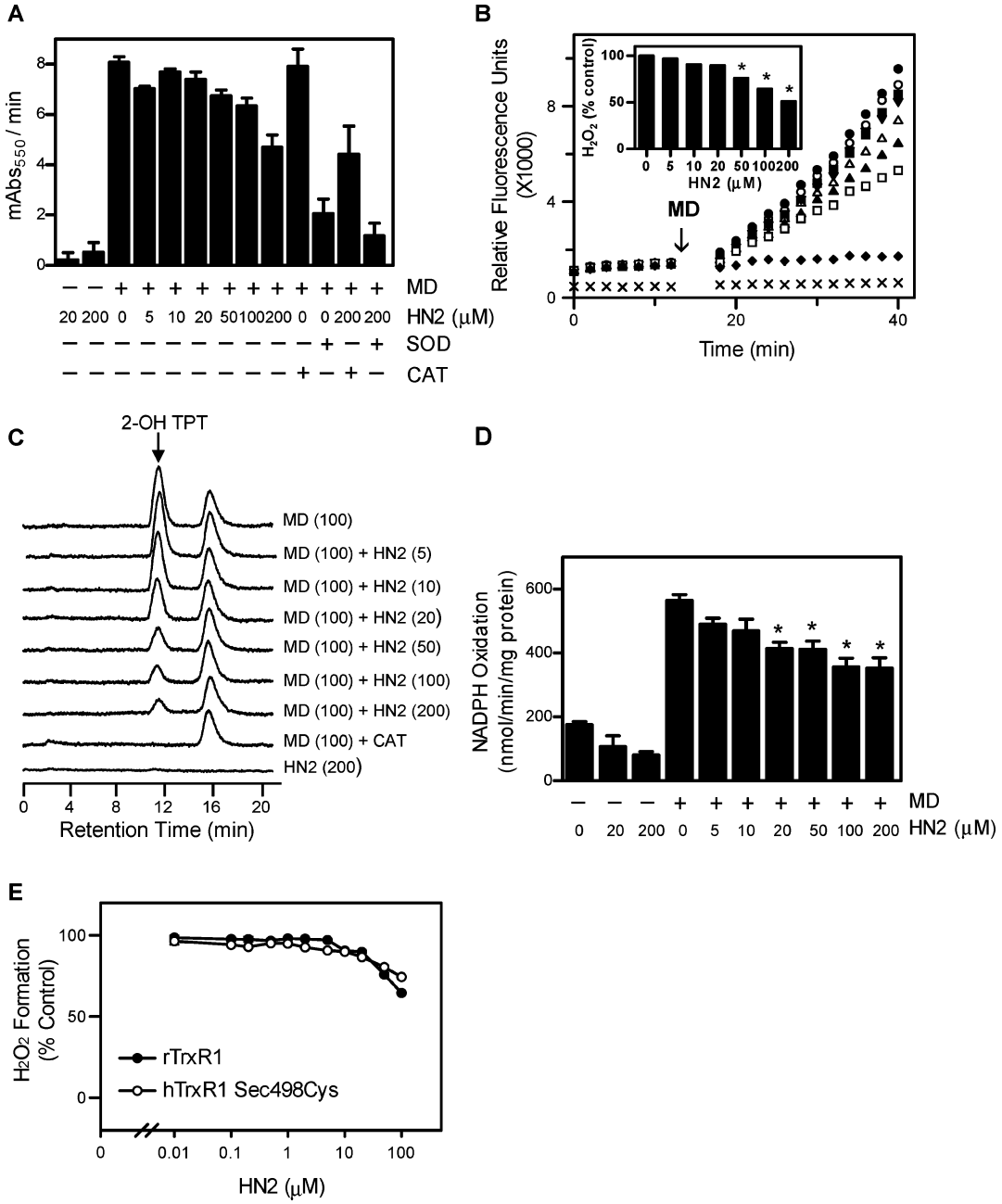

Figure 7. Effects of NH2 on menadione redox cycling by TrxR. (A) Effects of HN2 on menadione-generated superoxide anion production by purified rat TrxR. Superoxide anion was measured by the reduction of acetylated cytochrome c in the absence or presence of 100 μM menadione (MD). Some experiments also contained superoxide dismutase (SOD) or catalase (CAT). (B) Effects of HN2 on menadione-generated H_2O_2 by purified rat TrxR. TrxR was incubated with increasing concentrations of HN2 or vehicle control. The production of H_2O_2 was monitored using the Amplex Red assay. After 12 min, 100 μM menadione or vehicle control was added to the reaction mixture, and H_2O_2 formation was monitored continuously for an additional 22 min: (●) 0 μM HN2, (○) 5 μM HN2, (■) 10 μM HN2, (▼) 20 μM HN2, (Δ) 50 μM HN2, (▲) 100 μM HN2, (□) 200 μM HN2, and (×) 200 μM HN2 + catalase. The vehicle control sample (♦) without menadione was also treated with 200 μM HN2. The inset shows the effects of HN2 on menadione-generated H_2O_2 compared to vehicle-treated TrxR. (C) Effects of HN2 on menadione-generated hydroxyl radicals by purified rat TrxR. Hydroxyl radicals were measured using the terephthalate assay and the product, 2-hydroxyl terephthalate (2-OH TPT), was analyzed by HPLC. The concentrations of menadione and HN2 shown in parentheses are in micromolar. (D) Effects of HN2 on menadione-stimulated NADPH oxidation. NADPH utilization was followed by decreases in absorbance at 340 nm in the absence or presence of menadione (100 μM). Data are expressed as the mean ± SE (n = 3). * indicates significantly different ($p < 0.05$) from vehicle-treated control. (E) Menadione redox cycling mediated by TrxR pretreated with HN2. Reduced rat TrxR1 and human TrxR1 Sec498Cys mutant enzyme were treated with HN2 or vehicle control. After 30 min, menadione (100 μM) was added to reaction mix, and H_2O_2 formation was monitored using Amplex Red assay. Data are presented as percent of vehicle-treated samples.

in the other subunit. These results indicate that HN2 can inactivate TrxR by cross-linking catalytic residues, a process that involves HN2 substituting for a disulfide and/or selenosulfide, which is required for catalytic activity. In contrast to CEES, which selectively modifies the C-terminal redox center of TrxR,[25] HN2 alkylates both N- and C-terminal redox

dx.doi.org/10.1021/tx400329a | Chem. Res. Toxicol. 2014, 27, 61−75

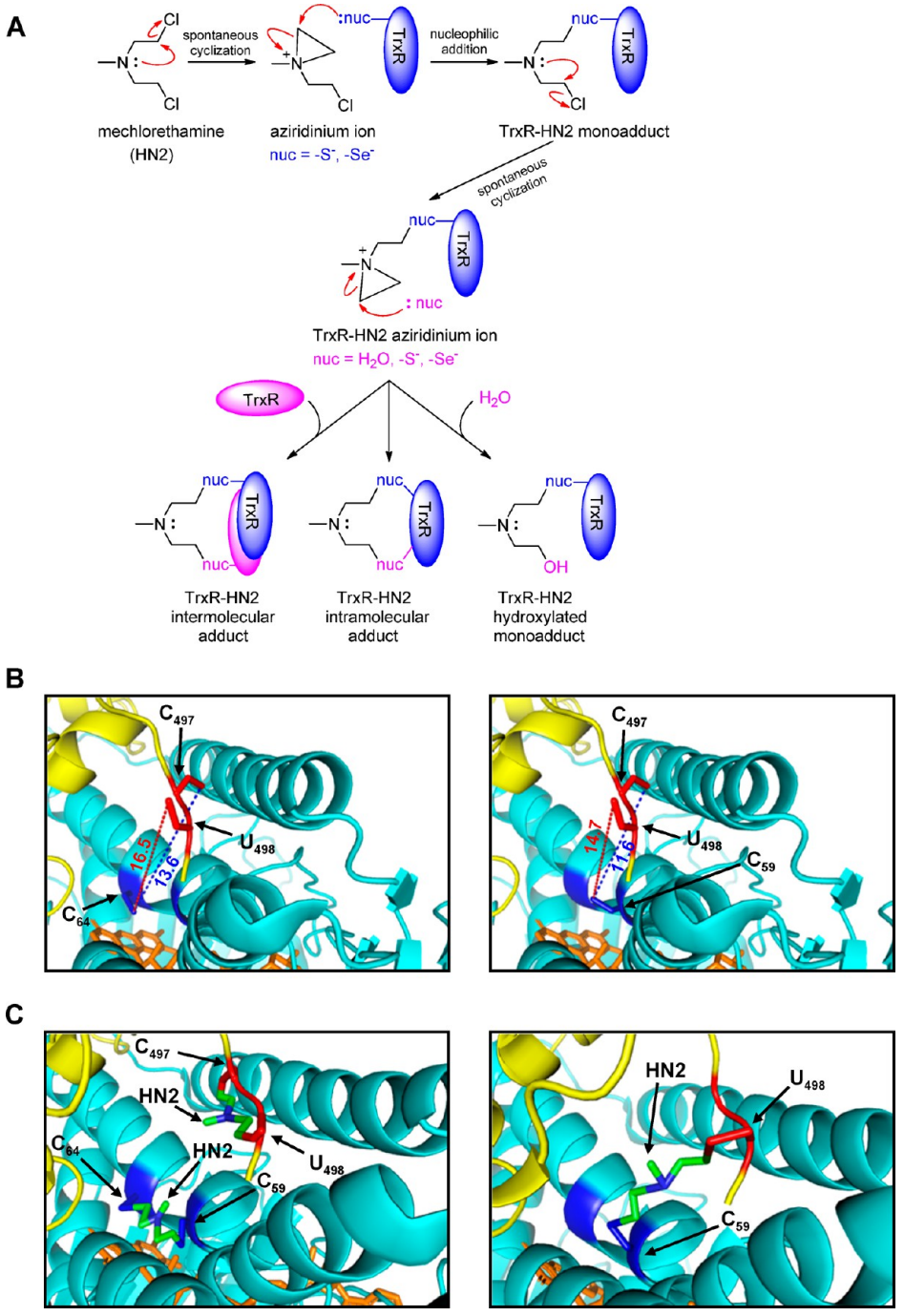

Figure 8. Molecular models for the formation of TrxR adducts with mechlorethamine. (A) Proposed mechanisms for the reaction of HN2 with TrxR. Under physiological conditions, HN2 spontaneously cyclizes by nucleophilic attack of nitrogen on the β-carbon adjacent chlorine, forming an aziridinium cation. This highly reactive intermediate undergoes further nucleophilic addition by adjacent nucleophiles such as nucleophilic sites on TrxR (including thiolate and selenolate groups within TrxR) to form TrxR−HN2 monoadducts. These intermediates are capable of cyclizing to form another aziridinium cation and react further by nucleophilic addition to form TrxR-hydroxyl HN2 monoadducts and TrxR−HN2 intramolecular and TrxR−HN2 intermolecular adducts. (B) Stereo view of the reduced N- and C-terminal redox centers of rat TrxR1. Molecular models were based on the crystal structure of rat TrxR1 (PDI ID: 3EAN). One subunit is shown in yellow and the other, in cyan. N-terminal redox center (cysteine 59 and cysteine 64) is shown in blue, and C-terminal redox center (cysteine 497 and selenocysteine 498) is shown in red. FAD is shown in orange. The relative distances of redox centers are labeled. (C) Models for TrxR complexed with HN2. Left panel shows that HN2 alkylated to the N- and C-terminal redox centers, respectively, causing intramolecular cross-links. Right panel shows that HN2 modified cysteine 59 in one subunit and selenocysteine 498 in the other subunit. This resulted in an intermolecular cross-link in the two subunits of the TrxR dimer.

domains in TrxR, which, as indicated, may contribute to the greater potency of this vesicant when compared to CEES. HN2 alkylation is known to cause structural distortions on target molecules, contributing to alterations in their biological activities.[41] For example, molecular modeling studies demonstrated that mechlorethamine treatment caused a high degree of DNA contortion, contributing to inhibition of DNA replication.[41] A 3D model of HN2 bound to TrxR on the

dx.doi.org/10.1021/tx400329a | Chem. Res. Toxicol. 2014, 27, 61−75

basis of the crystal structure of the enzyme and our LC−MS/MS analysis is shown in Figure 8B,C. Of note, catalytic residues in both the N- and C-terminal redox centers, including the cysteine 59/cysteine 64 pair and the cysteine 497/selenolcysteine 498 pair, are in close proximity in the unmodified enzyme, suggesting a favorable reaction for an intramolecular cross-link. The crystal structure also revealed that the distance between catalytic residues on the N- (dithiols) and C-terminal (selenothiol) redox centers of adjacent subunits is around 11−17 Å (Figure 8B), which is greater than the size of an extended HN2 molecule (7.5 Å).[41] This suggests that TrxR dimerization in the presence of HN2 may trigger a localized conformational change that allows the two targets to be in closer proximity. This interferes with substrate binding and blocks disulfide reduction by the enzyme. These results also indicate that bifunctional alkylating agents like HN2 can provide structural information that confirms the crystal structure of TrxR using a solution-based technique.

The preference of alkylation sites on cysteine is consistent with previous studies showing that different nitrogen mustards predominantly react with the thiolate side chain of cysteine residues within proteins.[23,29,42,43] Our BIAM experiments showed that treatment of oxidized TrxR with HN2 blocks iodoacetamide binding at pH 8.5 in a concentration-dependent manner, confirming that noncatalytic cysteine residues are also targets for HN2 modification. This is supported by our LC−MS/MS analysis that showed that HN2 covalently binds to other cysteine residues in TrxR including cysteine 177, 189, 382, and 383. On the basis of the crystal structure of the enzyme, these residues appear to be located in solvent-accessible regions, confirming that they can serve as targets for HN2 alkylation. At the present time, the functional significance of these cysteine adducts is not clear. Our findings that treatment of oxidized TrxR with HN2 has no significant effect on enzymatic activity and that no dimers/oligomers formation was detected in our BIAM-labeling experiment suggest that modification of cysteine residues other than those in catalytic centers may not contribute to enzyme inhibition and/or TrxR dimerization.

Of interest was our finding that HN2 can generate TrxR dimers and/or oligomers with purified enzyme, in type II epithelial cells, and in rat lung. In cell lysates isolated from A549 cells, additional higher-molecular-weight TrxR bands also appeared, which likely represent TrxR dimers bound to neighboring proteins. This is consistent with earlier studies showing that bifunctional electrophiles agents including HN2 can alkylate thioredoxin and thioredoxin-redox partners, such as peroxiredoxins and TrxR, forming high molecular cross-links in cells.[23] The mechanism mediating the formation of TrxR oligomers is not clear because we have been unable to detect additional HN2 cross-links between dimers and oligomers in the purified enzyme system. This may be due to methodological limitations of our LC−MS/MS analysis because larger peptides in the oligomers may have low ionization efficiency. Stable noncovalently linked tetrameric forms of TrxR have been observed in preparations of enzyme from human T-cells and rat liver as well as from recombinant expression of rat TrxR1 in *Escherichia coli*.[44,45] Studies on different forms of recombinant rat TrxR have shown that tetrameric TrxR is disulfide- or selenenylsulfide-linked and the dimeric and tetrameric forms of the enzyme have only half of the activity per subunit compared to homodimeric TrxR.[45] These observations imply that HN2 may cross-link residues critical in forming disulfide- or selenenylsulfide-linked tetramers, leading to cross-linked oligomers. It is known that the C-terminal redox center of TrxR is located in a conformationally flexible and solvent-accessible region of the enzyme,[34] which may allow the formation of an intermolecular cross-link by HN2 between two C-terminal catalytic sites from two adjacent molecules. Thus, it is possible that oligomer formation results from a cross-link between two C-terminal redox centers that are already cross-linked with N-terminal cysteine residues. In addition, structurally accessible cysteine residues in two cross-linked dimers may react with HN2 to form an oligomer. Further studies are needed to characterize more precisely the mechanisms by which HN2 induces TrxR oligomerization.

In addition to functioning as a disulfide reductase, TrxR also has prooxidant activity under certain conditions. The enzyme is known to catalyze the one-electron reduction of selected TrxR inhibitors including quinones, nitroaromatics, and bipyridyl herbicides, leading to generation of superoxide anion and induction of NADPH oxidase activity of TrxR.[5−7,12] Previous studies have demonstrated that the N-terminal dithiol motif and flavin binding site of TrxR but not the C-terminal selenothiol motif play important roles in superoxide anion generation by the enzyme.[46] Thus, variants of TrxR with Cys59Ser and/or Cys64Ser mutations display reduced superoxide anion generation and NADPH oxidase activity. Our data indicate that although HN2 is an effective inhibitor for TrxR disulfide reductase activity it only causes a small decrease in menadione redox cycling. This decrease is presumably due to the fact that HN2 can alkylate cysteine 59 and cysteine 64 in the N-terminal redox center of the enzyme. This is in agreement with findings with other inhibitors including auranofin that cause decreases in the formation of superoxide anion and hydroxyl radicals mediated by TrxR.[46] The differential effects of HN2 on disulfide reduction and chemical redox cycling suggest that TrxR mediates these reactions via distinct mechanisms. It is likely that redox cycling occurs on sites on the enzyme in proximity to the flavin that are not modified by HN2. Further studies are needed to identify these sites and to distinguish them from sites mediating disulfide reduction. We reported previously that CEES stimulated TrxR-mediated menadione redox cycling.[25] CEES is known to selectively modify the C-terminal selenocysteine motif of TrxR, which is not critical for chemical redox cycling.[25,46] The distinct effects of HN2 on TrxR-catalyzed chemical redox cycling may be the result of the vesicant also binding to the N-terminal redox motif of TrxR and forming both intra- and intermolecular cross-links in addition to alkylating the C-terminal redox motif of the enzyme.

Inhibition of TrxR has been shown to deplete cells of reduced thioredoxin, a critical disulfide reductase important in DNA synthesis and repair, and in maintaining the integrity of many redox-sensitive signaling molecules and proteins.[1,4] Moreover, both thioredoxin and TrxR function as antioxidants and can directly scavenge reactive oxygen species.[47,48] Interfering with these processes can result in disruption of antioxidant balance and initiate oxidative stress. Modification of selenocysteine in the C-terminal redox center of TrxR by different classes of electrophiles has been reported to be required for induction of apoptosis and necrosis.[8,9,49] Animal studies have shown that sulfur mustard vesicants induce apoptosis in both lung and skin.[50,51] Alkylation of TrxR by HN2 and consequent inhibition of enzyme activity in lung

epithelial cells may play a role in apoptosis and necrosis, a process that may also contribute to HN2-induced toxicity.

■ ASSOCIATED CONTENT

Supporting Information

Characterization of one monohydroxyl HN2 adduct and two intramolecular HN2 adducts identifed from a database search (summarized in Table 1). LC−MS/MS analysis of HN2-adducted TrxR tryptic peptide at *m/z* 554.63, 741.60, and 975.10. This material is available free of charge via the Internet at http://pubs.acs.org.

■ AUTHOR INFORMATION

Corresponding Author

*Tel.: 848-445-0170; Fax: 732-445-0119; E-mail: jlaskin@eohsi.rutgers.edu.

Funding

This work was supported in part by National Institutes of Health grants ES005022 (J.D.L. and D.L.L.), ES004738 (D.L.L. and J.D.L.), CA132624 (D.L.L. and J.D.L.), AR055073 (J.D.L., D.L.L., and D.E.H.), F32ES017389 (Y.J.), and GM034310 (D.L.L. and J.D.L.). This work was also funded in part by the National Institutes of Health CounterACT Program through the National Institute of Arthritis and Musculoskeletal and Skin Diseases (award U54AR055073 to J.D.L.). The contents are solely the responsibility of the authors and do not necessarily represent the official views of the federal government.

Notes

The authors declare no competing financial interest.

■ ABBREVIATIONS USED

HN2, mechlorethamine; TrxR, thioredoxin reductase; DTNB, 5,5′-dithiobis(2-nitrobenzoic acid); CEES, 2-chloroethyl ethyl sulfide; H_2O_2, hydrogen peroxide; BIAM, *N*-(biotinoyl)-*N*′-(iodoacetyl) ethylenediamine; DMEM, Dulbecco's modified Eagle's medium; HRP, horseradish peroxidase; ECL, chemiluminescence

■ REFERENCES

(1) Gromer, S., Urig, S., and Becker, K. (2004) The thioredoxin system−from science to clinic. *Med. Res. Rev. 24*, 40−89.
(2) Arner, E. S. (2009) Focus on mammalian thioredoxin reductases−important selenoproteins with versatile functions. *Biochim. Biophys. Acta 1790*, 495−526.
(3) Powis, G., and Kirkpatrick, D. L. (2007) Thioredoxin signaling as a target for cancer therapy. *Curr. Opin. Pharmacol. 7*, 392−397.
(4) Lu, J., and Holmgren, A. (2012) Thioredoxin system in cell death progression. *Antioxid. Redox Signaling 17*, 1738−1747.
(5) Cenas, N., Nivinskas, H., Anusevicius, Z., Sarlauskas, J., Lederer, F., and Arner, E. S. (2004) Interactions of quinones with thioredoxin reductase: A challenge to the antioxidant role of the mammalian selenoprotein. *J. Biol. Chem. 279*, 2583−2592.
(6) Cenas, N., Prast, S., Nivinskas, H., Sarlauskas, J., and Arner, E. S. (2006) Interactions of nitroaromatic compounds with the mammalian selenoprotein thioredoxin reductase and the relation to induction of apoptosis in human cancer cells. *J. Biol. Chem. 281*, 5593−5603.
(7) Gray, J. P., Heck, D. E., Mishin, V., Smith, P. J., Hong, J. Y., Thiruchelvam, M., Cory-Slechta, D. A., Laskin, D. L., and Laskin, J. D. (2007) Paraquat increases cyanide-insensitive respiration in murine lung epithelial cells by activating an NAD(P)H:paraquat oxidoreductase: Identification of the enzyme as thioredoxin reductase. *J. Biol. Chem. 282*, 7939−7949.
(8) Anestal, K., and Arner, E. S. (2003) Rapid induction of cell death by selenium-compromised thioredoxin reductase 1 but not by the fully active enzyme containing selenocysteine. *J. Biol. Chem. 278*, 15966−15972.
(9) Anestal, K., Prast-Nielsen, S., Cenas, N., and Arner, E. S. (2008) Cell death by SecTRAPs: Thioredoxin reductase as a prooxidant killer of cells. *PLoS One 3*, e1846-1−e1846-16.
(10) Witte, A. B., Anestal, K., Jerremalm, E., Ehrsson, H., and Arner, E. S. (2005) Inhibition of thioredoxin reductase but not of glutathione reductase by the major classes of alkylating and platinum-containing anticancer compounds. *Free Radical Biol. Med. 39*, 696−703.
(11) Wang, X., Zhang, J., and Xu, T. (2007) Cyclophosphamide as a potent inhibitor of tumor thioredoxin reductase in vivo. *Toxicol. Appl. Pharmacol. 218*, 88−95.
(12) Nordberg, J., Zhong, L., Holmgren, A., and Arner, E. S. (1998) Mammalian thioredoxin reductase is irreversibly inhibited by dinitrohalobenzenes by alkylation of both the redox active selenocysteine and its neighboring cysteine residue. *J. Biol. Chem. 273*, 10835−10842.
(13) Fang, J., and Holmgren, A. (2006) Inhibition of thioredoxin and thioredoxin reductase by 4-hydroxy-2-nonenal in vitro and in vivo. *J. Am. Chem. Soc. 128*, 1879−1885.
(14) Myers, C. R., and Myers, J. M. (2009) The effects of acrolein on peroxiredoxins, thioredoxins, and thioredoxin reductase in human bronchial epithelial cells. *Toxicology 257*, 95−104.
(15) Lu, J., Chew, E. H., and Holmgren, A. (2007) Targeting thioredoxin reductase is a basis for cancer therapy by arsenic trioxide. *Proc. Natl. Acad. Sci. U.S.A. 104*, 12288−12293.
(16) Myers, J. M., and Myers, C. R. (2009) The effects of hexavalent chromium on thioredoxin reductase and peroxiredoxins in human bronchial epithelial cells. *Free Radical Biol. Med. 47*, 1477−1485.
(17) Carvalho, C. M., Chew, E. H., Hashemy, S. I., Lu, J., and Holmgren, A. (2008) Inhibition of the human thioredoxin system. A molecular mechanism of mercury toxicity. *J. Biol. Chem. 283*, 11913−11923.
(18) Moos, P. J., Edes, K., Cassidy, P., Massuda, E., and Fitzpatrick, F. A. (2003) Electrophilic prostaglandins and lipid aldehydes repress redox-sensitive transcription factors p53 and hypoxia-inducible factor by impairing the selenoprotein thioredoxin reductase. *J. Biol. Chem. 278*, 745−750.
(19) Gromer, S., Johansson, L., Bauer, H., Arscott, L. D., Rauch, S., Ballou, D. P., Williams, C. H., Jr., Schirmer, R. H., and Arner, E. S. (2003) Active sites of thioredoxin reductases: Why selenoproteins? *Proc. Natl. Acad. Sci. U.S.A. 100*, 12618−12623.
(20) Zhong, L., Arner, E. S., and Holmgren, A. (2000) Structure and mechanism of mammalian thioredoxin reductase: The active site is a redox-active selenolthiol/selenenylsulfide formed from the conserved cysteine-selenocysteine sequence. *Proc. Natl. Acad. Sci. U.S.A. 97*, 5854−5859.
(21) Arner, E. S. (2010) Selenoproteins−What unique properties can arise with selenocysteine in place of cysteine? *Exp. Cell Res. 316*, 1296−1303.
(22) Fang, J., Lu, J., and Holmgren, A. (2005) Thioredoxin reductase is irreversibly modified by curcumin: A novel molecular mechanism for its anticancer activity. *J. Biol. Chem. 280*, 25284−25290.
(23) Naticchia, M. R., Brown, H. A., Garcia, F. J., Lamade, A. M., Justice, S. L., Herrin, R. P., Morano, K. A., and West, J. D. (2013) Bifunctional electrophiles cross-link thioredoxins with redox relay partners in cells. *Chem. Res. Toxicol. 26*, 490−497.
(24) Ghanei, M., and Harandi, A. A. (2007) Long term consequences from exposure to sulfur mustard: A review. *Inhalation Toxicol. 19*, 451−456.
(25) Jan, Y. H., Heck, D. E., Gray, J. P., Zheng, H., Casillas, R. P., Laskin, D. L., and Laskin, J. D. (2010) Selective targeting of selenocysteine in thioredoxin reductase by the half mustard 2-chloroethyl ethyl sulfide in lung epithelial cells. *Chem. Res. Toxicol. 23*, 1045−1053.
(26) Rajski, S. R., and Williams, R. M. (1998) DNA cross-linking agents as antitumor drugs. *Chem. Rev. 98*, 2723−2796.
(27) Sunil, V. R., Patel, K. J., Shen, J., Reimer, D., Gow, A. J., Laskin, J. D., and Laskin, D. L. (2011) Functional and inflammatory

alterations in the lung following exposure of rats to nitrogen mustard. *Toxicol. Appl. Pharmacol. 250*, 10−18.
(28) Holmgren, A., and Bjornstedt, M. (1995) Thioredoxin and thioredoxin reductase. *Methods Enzymol. 252*, 199−208.
(29) Thompson, V. R., and Decaprio, A. P. (2013) Covalent adduction of nitrogen mustards to model protein nucleophiles. *Chem. Res. Toxicol. 26*, 1263−1271.
(30) Rubino, F. M., Pitton, M., Di Fabio, D., and Colombi, A. (2009) Toward an "omic" physiopathology of reactive chemicals: Thirty years of mass spectrometric study of the protein adducts with endogenous and xenobiotic compounds. *Mass Spectrom. Rev. 28*, 725−784.
(31) Boveris, A., Alvarez, S., Bustamante, J., and Valdez, L. (2002) Measurement of superoxide radical and hydrogen peroxide production in isolated cells and subcellular organelles. *Methods Enzymol. 349*, 280−287.
(32) Mishin, V. M., and Thomas, P. E. (2004) Characterization of hydroxyl radical formation by microsomal enzymes using a water-soluble trap, terephthalate. *Biochem. Pharmacol. 68*, 747−752.
(33) DeLano, W. L. (2002) *The PyMOL molecular graphics system*, DeLano Scientific, San Carlos, CA, http://www.pymol.org.
(34) Cheng, Q., Sandalova, T., Lindqvist, Y., and Arner, E. S. (2009) Crystal structure and catalysis of the selenoprotein thioredoxin reductase 1. *J. Biol. Chem. 284*, 3998−4008.
(35) Chew, E. H., Lu, J., Bradshaw, T. D., and Holmgren, A. (2008) Thioredoxin reductase inhibition by antitumor quinols: A quinol pharmacophore effect correlating to antiproliferative activity. *FASEB J. 22*, 2072−2083.
(36) Arner, E. S. (1999) Superoxide production by dinitrophenyl-derivatized thioredoxin reductase–a model for the mechanism and correlation to immunostimulation by dinitrohalobenzenes. *BioFactors 10*, 219−226.
(37) Rigobello, M. P., Vianello, F., Folda, A., Roman, C., Scutari, G., and Bindoli, A. (2006) Differential effect of calcium ions on the cytosolic and mitochondrial thioredoxin reductase. *Biochem. Biophys. Res. Commun. 343*, 873−878.
(38) Rackham, O., Shearwood, A. M., Thyer, R., McNamara, E., Davies, S. M., Callus, B. A., Miranda-Vizuete, A., Berners-Price, S. J., Cheng, Q., Arner, E. S., and Filipovska, A. (2011) Substrate and inhibitor specificities differ between human cytosolic and mitochondrial thioredoxin reductases: Implications for development of specific inhibitors. *Free Radical Biol. Med. 50*, 689−699.
(39) Biterova, E. I., Turanov, A. A., Gladyshev, V. N., and Barycki, J. J. (2005) Crystal structures of oxidized and reduced mitochondrial thioredoxin reductase provide molecular details of the reaction mechanism. *Proc. Natl. Acad. Sci. U.S.A. 102*, 15018−15023.
(40) Tonissen, K. F., and Di Trapani, G. (2009) Thioredoxin system inhibitors as mediators of apoptosis for cancer therapy. *Mol. Nutr. Food Res. 53*, 87−103.
(41) Rink, S. M., and Hopkins, P. B. (1995) A mechlorethamine-induced DNA interstrand cross-link bends duplex DNA. *Biochemistry 34*, 1439−1445.
(42) Loeber, R. L., Michaelson-Richie, E. D., Codreanu, S. G., Liebler, D. C., Campbell, C. R., and Tretyakova, N. Y. (2009) Proteomic analysis of DNA-protein cross-linking by antitumor nitrogen mustards. *Chem. Res. Toxicol. 22*, 1151−1162.
(43) Antoine, M., Fabris, D., and Fenselau, C. (1998) Covalent sequestration of the nitrogen mustard mechlorethamine by metallothionein. *Drug Metab. Dispos. 26*, 921−926.
(44) Gladyshev, V. N., Jeang, K. T., and Stadtman, T. C. (1996) Selenocysteine, identified as the penultimate C-terminal residue in human T-cell thioredoxin reductase, corresponds to TGA in the human placental gene. *Proc. Natl. Acad. Sci. U.S.A. 93*, 6146−6151.
(45) Rengby, O., Cheng, Q., Vahter, M., Jornvall, H., and Arner, E. S. (2009) Highly active dimeric and low-activity tetrameric forms of selenium-containing rat thioredoxin reductase 1. *Free Radical Biol. Med. 46*, 893−904.
(46) Cheng, Q., Antholine, W. E., Myers, J. M., Kalyanaraman, B., Arner, E. S., and Myers, C. R. (2010) The selenium-independent inherent pro-oxidant NADPH oxidase activity of mammalian thioredoxin reductase and its selenium-dependent direct peroxidase activities. *J. Biol. Chem. 285*, 21708−21723.
(47) Das, K. C., and Das, C. K. (2000) Thioredoxin, a singlet oxygen quencher and hydroxyl radical scavenger: Redox independent functions. *Biochem. Biophys. Res. Commun. 277*, 443−447.
(48) Zhong, L., and Holmgren, A. (2000) Essential role of selenium in the catalytic activities of mammalian thioredoxin reductase revealed by characterization of recombinant enzymes with selenocysteine mutations. *J. Biol. Chem. 275*, 18121−18128.
(49) Cassidy, P. B., Edes, K., Nelson, C. C., Parsawar, K., Fitzpatrick, F. A., and Moos, P. J. (2006) Thioredoxin reductase is required for the inactivation of tumor suppressor p53 and for apoptosis induced by endogenous electrophiles. *Carcinogenesis 27*, 2538−2549.
(50) Malaviya, R., Sunil, V. R., Cervelli, J., Anderson, D. R., Holmes, W. W., Conti, M. L., Gordon, R. E., Laskin, J. D., and Laskin, D. L. (2010) Inflammatory effects of inhaled sulfur mustard in rat lung. *Toxicol. Appl. Pharmacol. 248*, 89−99.
(51) Kan, R. K., Pleva, C. M., Hamilton, T. A., Anderson, D. R., and Petrali, J. P. (2003) Sulfur mustard-induced apoptosis in hairless guinea pig skin. *Toxicol. Pathol. 31*, 185−190.